An amide based polyvinyl alcohol / protic ionic liquid (PVA / PIL) gel electrolyte for supercapacitor applications

Chandrasekaran Ramasamy, Patrice Porion, Laure Timperman, Mérièm Anouti

An amide based polyvinyl alcohol / protic ionic liquid (PVA / PIL) gel electrolyte for supercapacitor applications

Ramasamy Chandrasekaran [a,b*], Patrice Porion[c], Laure Timperman[a], Mérièm Anouti[a]

[a] *Physicochimie des Matériaux et Electrolytes pour l'énergie (PCM2E), EA 6299, Université F. Rabelais de Tours, Parc de Grandmont, 37200 Tours, France.*
[b] *Le STUDIUM Fellow, Loire Valley Institute for Advanced Studies, 1 rue Dupanloup, 45000 Orléans – France*
[c] *ICMN CNRS - Université d'Orléans, UMR 7374, 1b rue de la Férollerie, 45071 Orléans Cedex 02, France*

ABSTRACT

An aqueous gel based on polyvinyl alcohol (PVA) and a mixture of two nitrate salts, namely lithium nitrate ($LiNO_3$) and pyrrolidinium nitrate, PIL ($PyrrNO_3$) was prepared and used as an electrolyte. The gel electrolyte shows a high conductivity in the presence of formamide (FMD), which was studied as an organic additive in the gel at 5 to 400 % with respect to the salt content. Their electrochemical behaviors were examined by cyclic voltammetry, galvanostatic charge-discharge and an impedance technique at room temperature (17°C). The 100 % of amide in the gel has shown a maximum ionic conductivity of 33 x 10^{-3} and 11.2 x 10^{-3} Scm^{-1} at 17°C and -20°C respectively. A two electrode supercapacitor (SC) was assembled and analyzed. The cycle life is improved by the additive over the bare gel, as evidenced by the galvanostatic cycling. The specific discharge capacitance of SC based on the 100% of amide can be used for delivering 34.2, 27.3 and 21 Fg^{-1} at 1.5 V under a constant current density of 50, 100 and 500 mAg^{-1} respectively. Moreover, the SC efficiency was maintained at 95%, and above as well as the capacity loss was minimized in the presence of the additive. This quasi solid-state supercapacitor will be capable of delivering an energy density of 12-13 $Whkg^{-1}$and maximum power density of 0.60 $kWkg^{-1}$ at 2 V. The results confirm that the capacitive enhancement is at the lower limit of the FMD.

Keywords
Polyvinyl alcohol gel; Activated Carbon, supercapacitor: formamide; specific energy

* Corresponding author (Present)
chandruanna@yahoo.com (Ramasamy Chandrasekaran)

1. Introduction

Electrochemical energy conversion based devices are an alternative power and energy storage devices in view of non renewable source limitations and also considering air-land pollutions. Many advanced energy storage systems exist in portable power systems. But the systems are still focusing for enhancements due to the rapid and urgency of energy demands. In this view, electric double layer capacitor (EDLC) which is one of the supercapacitor (SC) class has attracted for energy storage device due to its high power density and long life cycle [1, 2], but its practical energy density is around 10 $Whkg^{-1}$ only where its power density is superior to batteries likely 10 $kWkg^{-1}$. We can improve it by battery like materials through redox chemistry, but it affects the power density, which determines the cell life [3, 4].

Generally, porous carbon materials are the most used electrodes for SCs due to their high surface area and high specific capacity. The carbon is a safe, cost-effective and green material with the stable electrochemical mode of operations. The high surface area, pore volumes and pore size distributions of these activated carbon electrodes are significant physical properties that regulate the capacity of these devices to store energy [5]. However, the performance of SCs depends on electrolyte selection; an appropriate electrolyte according to the active material is necessary to improve the energy cell storage and its electrochemical performance [6]. The choice of electrolyte is related to its properties like its flammability, toxicity, its impact on the environment, conventional uses and also its transport properties. Furthermore, electrolyte depletion problems during charging due to the small electrolyte reservoir compared to the large surface area of the electrodes make it necessary to have a high concentration of the salts in the electrolyte. All of these requirements can be met with a gel electrolyte [7-9].

PVA is a well-known polymer matrix for portable energy storage applications [10, 11]. The gels have good electrical contact, safe, mechanical flexibility, as well as sealing way is lessened. The PVA is a hydrophilic polymer that has excellent film-forming, emulsifying, surfactant and adhesive properties, making it a strong contender for a variety of applications. Its weak conductivity, however, can be improved by introducing ionic solutes. The gels are to be considered as a medium to minimize cell self-discharge. To increase their electrochemical activities, a common way to support the stability of viscous gel is in the addition of a sufficient amount of salts and organic solvents as viscosity stabilizers [12]. A general approach to developing gels is to promote their conductivity or to mechanically plasticize the gels. The PVA

transition temperature, usually around 80°C, may be lowered by solvents or plasticizers. As a result, the crystallization level of the gel, generally around 0°C, can also be hindered [11]. Some organic additives are used for redox capabilities and as host supporting materials for the SC improvements. For a high voltage window, thermal stability and device safety, an ionic liquid (IL) is a good choice [7, 13, 14]. ILs, are room temperature molten salts, green electrolytes due to their physicochemical properties. As a sub-group of ILs, protic ionic liquids (PILs) are now emerging as versatile media for electrochemical devices [15]. The pyrrolidinium nitrate ($PyrrNO_3$) as PIL is easily soluble in water, a very good electrochemical activity because of its conductivity and potential window [16, 17]. We have presented in our previous works the effect of the amide additions as H-bond donor species in deep eutectic solvent (DES) formulations and their role in the SCs [14, 18], and here is an attempt of FMD to the PVA- PIL gel for SC uses.

Herein, we present the PVA gel preparations, their thermal and physical characterizations. An activated carbon (AC) electrode based SCs was studied in the gel by using cyclic voltammetry, galvanostatic cycling and impedance techniques. Emphasis was placed on the amide effect on the SC performance and diffusion mechanism of ions by Pulsed-Gradient Spin-Echo NMR (PGSE-NMR) method.

2. Material and method

The following starting materials were employed for the electrolyte formulation: Polyvinyl alcohol (PVA, $[CH_2CH(OH)]_n$; MW ≈ 7.4 x 10^4 $gmol^{-1}$), $LiNO_3$ salt (LS) and formamide (FMD, $[HCONH_2]$,Sigma Aldrich). The PIL, pyrrolidinium nitrate ($PyrrNO_3$)) was synthesized in accordance with our earlier reports [16, 17]. Appropriate weight ratios of the materials (PVA: PIL: $LiNO_3$ at 70:15:15%) were mixed in deionized water (30 ml) and stirred well about 3 hours at 80°. Finally, the obtained gel was allowed a day on stirring at room temperature for a perfect gelation. This gel polymer electrolyte (GPE) sample was indexed as S2. For a comparison, a GPE without PIL i.e, (PVA/ $LiNO_3$) (70:30) was prepared and assigned as S1, A system without PVA (PIL/FMD alone) at (0.15 g/30 ml) ratio were also prepared and indexed as SA. Following this, 25, 100, 200, and 400 weight percent of FMD with respect to the total salt weight (LS+PIL) were introduced together with the PVA gel and indexed as S3, S4, S5, and S6 respectively. The full detailed version is given in Table 1. Activated carbon (AC, 1500 m^2g^{-1}, Blue Solution Ltd.,) was used as SC electrodes (1 cm in diameter, 0.78 cm^2 in area and 4.5 mg as active material). The electrodes were prepared by manual mixing of AC, acetylene black (to improve the

electrical conductivity) and Poly(vinylidene fluoride), PVDF as a binder at weight ratio of 8:1:1 in the presence of a few drops of N methyl-2-pyrolidone (NMP) for a homogeneous slurry and kept at 80°C. The slurry was coated with aluminum foil as a current collector. A two electrode SC (Swagelok cell) was used with the gel soaked cellulose paper (thickness ≈ 90 microns). The SCs were analyzed at room temperature (17°C) in a common SC configuration of AC | GPE | AC.

Table 1. The GPE system formulations, abbreviations and its constitutes

Weight in g	Acronyms						
	SA	S1	S2	S3	S4	S5	S6
PVA	0	3.5	3.5	3.5	3.5	3.5	3.5
H_2O in ml	0	30	30	30	30	30	30
$LiNO_3$	0	1.5	1.5	1.5	1.5	1.5	1.5
$PyrNO_3$	1.5	0	0.75	0.75	0.75	0.75	0.75
FMD	30ml	0	0	0.36	1.5	3.0	6.0

Differential scanning calorimetry (DSC) was carried out on by using a Perkin-Elmer DSC 4000 under a nitrogen atmosphere, coupled with an Intracooler SP VLT 100. Samples for DSC measurements were sealed in aluminium pans. Four-probe DC conductivity measurements of the GPEs were conducted in our standard four electrode test cell (Biologic) in which plating electrodes served as the electrical contacts with ≈1mL of the gel.

The Pulsed-Gradient Spin-Echo NMR (PGSE-NMR) method [19] is used to measure the self-diffusion coefficient of a large variety of liquids and ionic species. Lithium self-diffusion coefficients was determined by lithium (^{7}Li) NMR. All the experiments were performed on a Bruker Avance DSX100 spectrometer with a 2.35T superconducting magnet, equipped with a 10-mm micro-imaging probe (Micro5 Bruker). The Larmor resonance frequency is 39.91 MHz for ^{7}Li nucleus. To improve the accuracy of the self-diffusion measurements, a modified stimulated spin-echo sequence (13-interval PGSTE pulse sequence with a bipolar gradient pair) was utilized. By using the PGSE-NMR method, self-diffusion coefficients were determined by measuring the decrease of the NMR echo signal intensity E through increasing magnetic field gradients (g). The self-diffusion coefficients, D, were then obtained by a simple linear least-squares fitting of the classic echo attenuation relationship according to Equation 1:

$$E(g,\Delta) = I(g, \Delta)/I(0,\Delta) = \exp [-\gamma^2 g^2 2\delta^2 D(\Delta-\delta/3)] \quad (1)$$

Where, I (g, Δ) and I (0, Δ) are the echo intensity which is measured with and without the field gradient *g* (varying between 0 and g_{max}). δ is its duration, γ is the gyromagnetic ratio of the nuclei, Δ is the diffusion time (fixed to 100 ms) and *D* is the self-diffusion coefficient. The magnetic field gradient duration δ was 4 ms, and the recovery delay was ranged from 60 s to 70 s depending on the longitudinal relaxation time T_1 of the sample. The maximum value of the magnetic field gradient (g_{max}) was set to 0.5T/m. The samples were prepared and placed in sealed glass tubes. For NMR measurements, samples were thermally equilibrated at 25°C during 30 min before any acquisition. Indeed, such experimental conditions allow a good homogeneity of the set point temperature across the whole samples.

A sequence of electrochemical experimental tests on the SCs was carried out in the following order (i) Electrochemical impedance spectroscopy (EIS), (ii) Cyclic voltammetry (CV) and (iii) Galvanostatic charge- discharge studies (CD) using a VMP 3 Electrochemical Analyzer, (Biologic, France). The EIS was recorded at open circuit potential (OCP) over the frequency range of 100 kHz to 0.01 Hz in a 2 mV amplitude and their corresponding specific capacitances C (Fg^{-1}) were calculated using the relation $C = -1/ (2\pi fZ''/m_t)$, where Z'' is the imaginary part of impedance (Ω) at 1 mHz frequency (f)), m_t is the weight of the two electrodes.

The CV experiments were performed in the potential range from 0 V to 2 V at 5 and 50 mVs^{-1} scan rates, and their corresponding gravimetric specific capacitances C (Fg^{-1}) were calculated using the equation $C = I/ (m_t.v)$, where I is an average peak value of the anodic-cathodic currents ($i_a+i_c/ 2$), m_t is the weight of the two electrodes and *v* is scan rate. Galvanostatic charge-discharge test (CD) was performed at various current densities, 50, 100, 250 and 500 $mA.g^{-1}$. Their corresponding specific capacitances C (Fg^{-1}) were obtained from the formula $C_{cal} = I\Delta t /\Delta V.m_t$, where I is the applied current, Δt is discharge time duration in seconds, m_t is the two electrode weight and ΔV is the potential window (specific capacity of each electrode, $C_{sp} = 4 \times C_{cal}$).

For evaluation of the SCs, the characterization of their energy density (E_{max}) and power density (P_{max}) were determined from the CD studies using $E = ½ CV^2$ and $P = V^2/4R$, respectively, where C is the specific capacitance from the total cell weight, R is the ESR of the cell which derives from a sudden potential drop at charge-discharge curves ($\Delta V_d/2I$ where ΔV_d is the voltage difference between the first two points of a discharge curve), V is the applied potential limit. Then, the E_{real} value was measured directly using the EC lab software tools, (E_{real}

means IR drop included, $P_{real}= E_{real}/\Delta t$ where Δt is the time taken between initial and final voltage limit). The reported capacitance values are based on the two electrode weight and the 2nd cycle is represented for CVs and CDs curves. Finally, in order to confirm the cell limit, the electrolyte voltage window was also checked from the CD in the range of 0-2.0 V

3. Results and discussion

3.1 Characterization of gel electrolyte

3.1.1 Thermal properties

As mentioned above, aqueous PVA-based gels are formed by mixing two salts ($LiNO_3$ and $PyrrNO_3$) and PVA. This mixture leads to the formation of a liquid gel phase by self-association via hydrogen bonds and coulombic interactions. The gel phase is generally characterized by a lower freezing point than aqueous electrolytes.

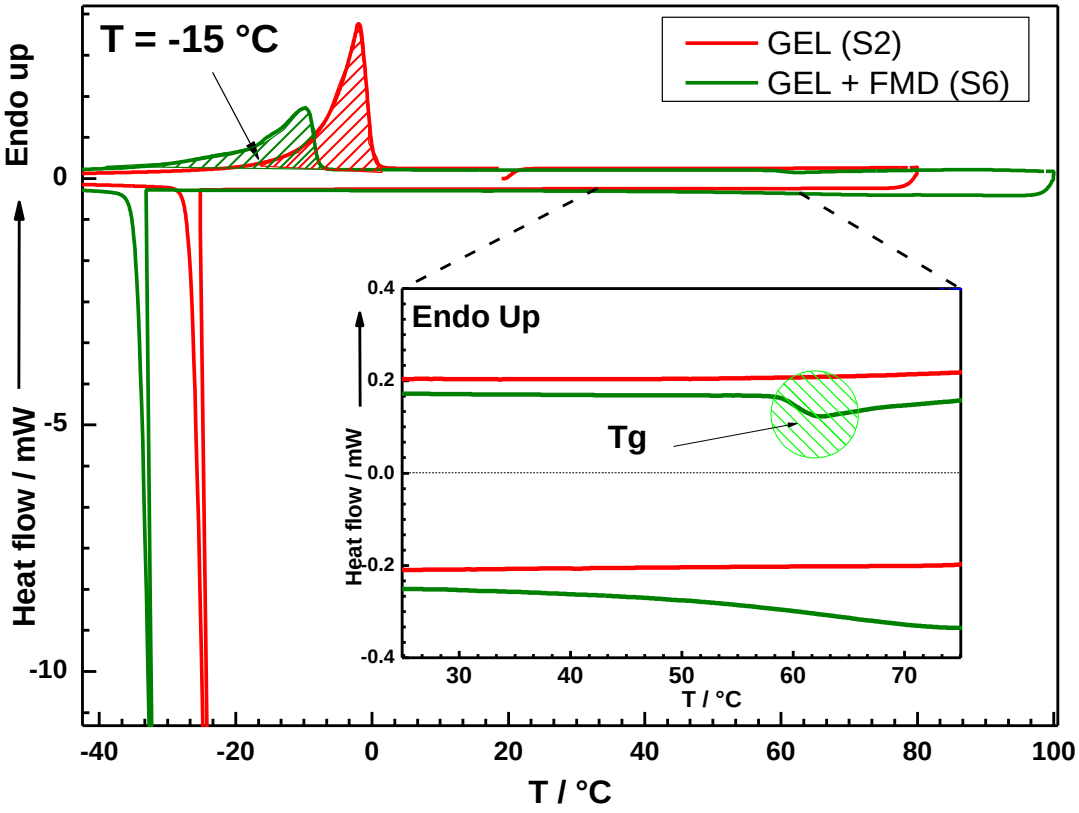

Fig.1 The DSC curve illustrations of S2 (without FMD) and S6 gels (with FMD)

Fig. 1 shows the comparative DSC curves of the PVA gel polymer electrolyte and gel with FMD, S2 and S6, respectively. As can be shown, the typical shouldered endothermic peak starting at -15°C corresponds to the melting of the host polymer PVA based gel in eutectic mixture with aqueous media. Blending with FMD lowers the melting point substantially to -30 °C. At the same time, the area of the melting peak reduces significantly. This is attributed to the large proportion of highly dissociated polar components that cause an increase in the amorphous content distributed in the overall material. A sharp exothermic crystallization peak at -25 °C and -30 °C has been observed for PVA gel without and with FMD, respectively, which is assigned to the entrapped water and water/FMD mixture with the host polymer PVA. The curve shows that the PVA interaction with the salt. Further, it may be noted that the GPE shows, in the presence of FMD, a lowering of its glass transition, Tg, by comparison with classical aqueous PVA gel (85°C). Finally, we can observe that the samples S2 and S6 remain stable in the same gel phase over a substantially wide temperature range from -10 to 100°C, for S2 and -20 to 100°C in the presence of FMD (S6), which is a required parameter of the SC.

3 .1.2 Transport properties

Conductivity

Fig. 2a represents the temperature dependent conductivity curves of the GPEs from -20 to 25°C in which a linear variation of conductivity such as an Arrhenius type of thermally activated process is observed at low temperature, but a small abrupt non-linearity was noticed which might be a crystalline form of PVA. As per thermodynamic aspects, the curves did not show a state of free water or bulk water, i.e., absence of a peak around the 0°C. There was a magnificent Arrhenius type behavior in the case of the amide based sample, S5 and PIL/FMD (SA) which had no abrupt change at low temperature region, which might be suppressed by the amide where as all other samples have the nonlinear behavior. Herein, a prevention of crystalline formation was hindered by the FMD. These results are consistent with the values observed by DSC. At 17°C, room temperature of electrochemical test, the conductivity values are 17.5, 24 and 33 $mScm^{-1}$ for S1, S2, and S5, respectively. It is interesting here is the low temperature conductivity value of the S5 which is still large enough to work as a good electrolyte system compared with S1 and S2 systems (12 $mScm^{-1}$ vs 1 $mScm^{-1}$) It is clearly

shown the changes on their conductivity values which confirms the role of high dielectric constitutes within it. Arrhenius region (ion hoping mechanisms as a main) was observed at in low temperature section while VTF type curved nature was started during the high temperatures. This ionic conductivity is associated with ion hopping and segmental motion increments from the combination of Arrhenius and VTF model behaviors respectively. The dielectric constants of the solvents are very important role in the conductivity enhancements through the ion dissociations and chain relaxations. Available free volume of the PVA altered by additives which leads to the increase of the segment motion.

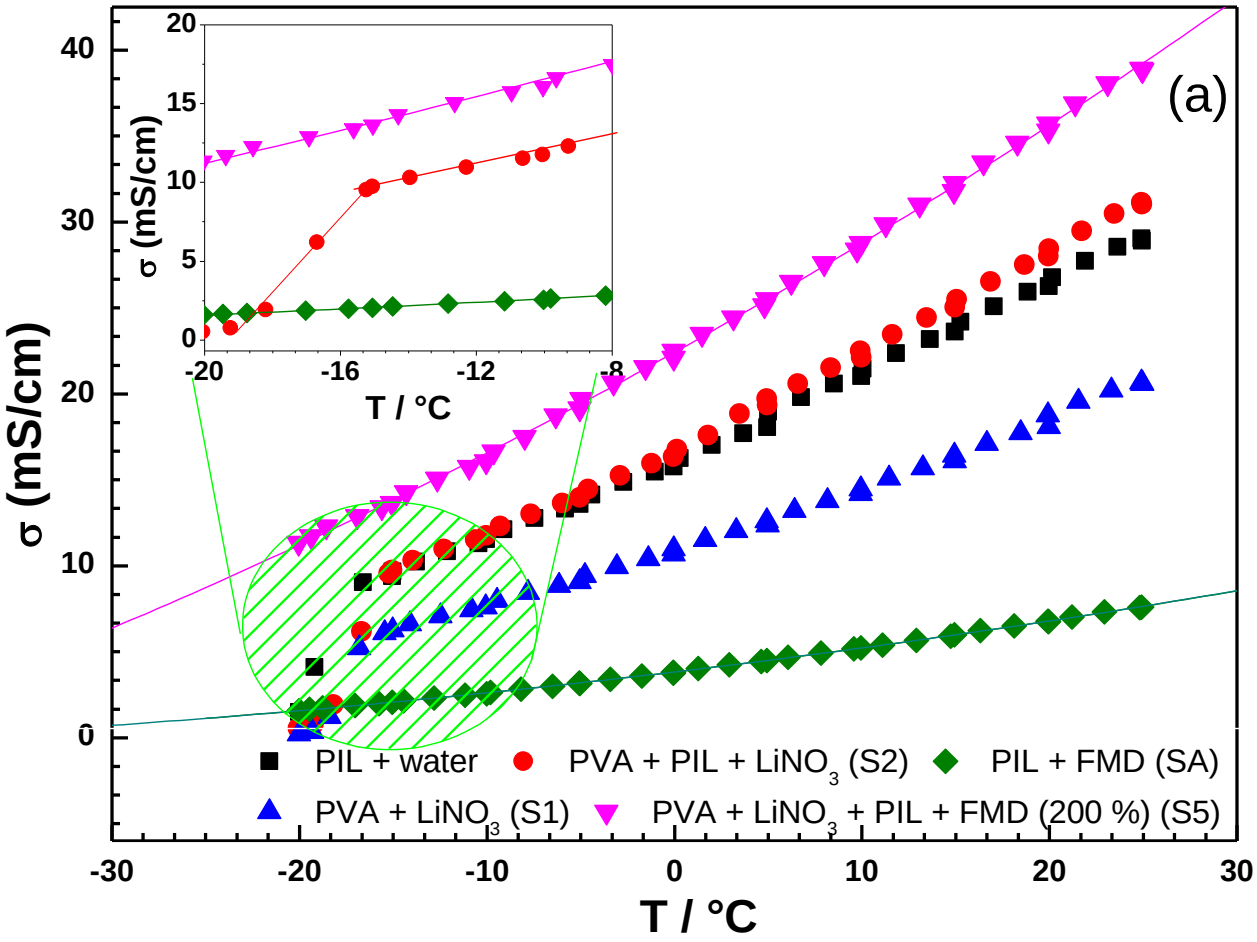

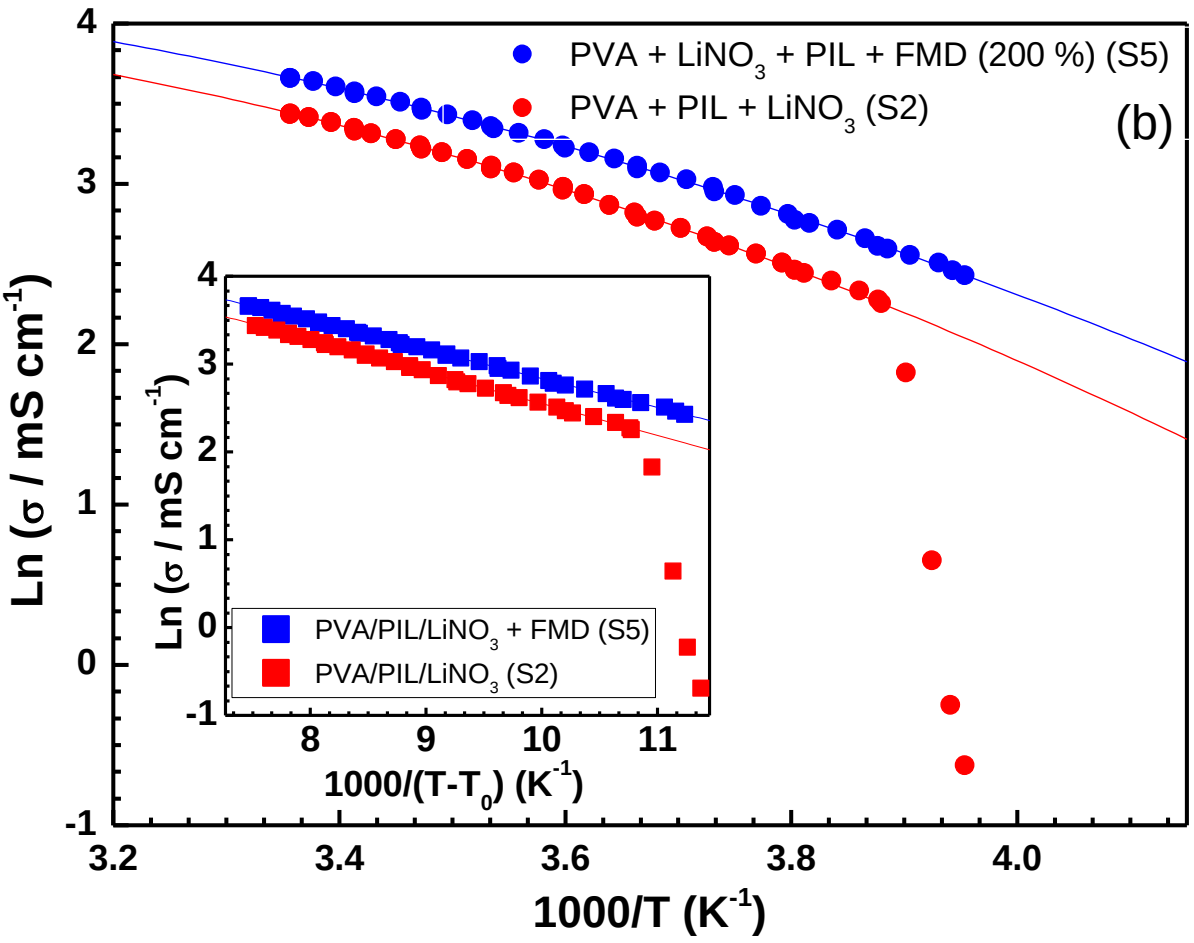

Fig. 2. The temperature dependent conductivity of the GPEs from -20 to 25°C (Fig.2a) and Fig. 2b for S2, S5 only

The effect of FMD in PVA gel is shown alone in Fig.2b to distinguish the behaviors. As seen in Fig 2b, with the non-linearity dependence of temperature with conductivity, it is clear that the gel electrolyte has a non-Arrhenius behavior (Eq 2), in the studied temperature domain. However, best fit (R = 0.999) of conductivity obtained with temperature according to the VTF (Vogel-Tamman-Fulcher)-like relationship (Eq 3), indicates that the ion mobility is coupled with the segmental motion of the polymer chain.

$$\sigma = \sigma_0 exp\left[\frac{-Ea}{R.T}\right] \qquad (2) \qquad \sigma = \sigma_0' exp\left[\frac{B}{T-T_0}\right] \qquad (3)$$

The fitting parameters as ideal temperature transition (T_0 = 165 K) and Pseudo-activation energy are B = (33 and 36)*R KJmol^{-1} for S6 and S2, respectively. We can note also, more precisely, in the VTF temperature-conductivity dependence curves, the crystallization for the sample without FMD.

Fig. 3 shows a schematic illustration of the different motilities of the ions present in the GPE matrix and the role of FMD is displaced in between the action of PVA chain and ionic species through inter and intra molecular actions. In addition, Grotthuss mechanism, as proton hopping mechanisms which involves a movement proton or proton defect moves in hydrogen bond network of water molecules or other hydrogen-bond liquids. We can justify the conductivities by Grotthuss mobility toward the jumping Li^+ and $Pyrr^+$ cations on the OH-bridge during the charge-discharge process with respect to SC electrode polarities. FMD can act as dissociating solvent for ion pair and at the same time as proton donor, A dissociation of both salts is easily obtainable due to their dielectric constant of the two proton donors here: H_2O (ε = 78) and FMD (ε = 111) as well as their solvation which is responsible for ionic motion [(H_2O) = 4.8 Debye; (FMD) = 3.3 Debye)]. FMD may be play to neutralize the OH group. By its role in the PVA gel matrix, the FMD facilitates the jump of labile proton as part of ion mobility, largely responsible for the high conductivity observed even at low temperature. In brief, FMD facilitates the solvated ion motions by its polarity.

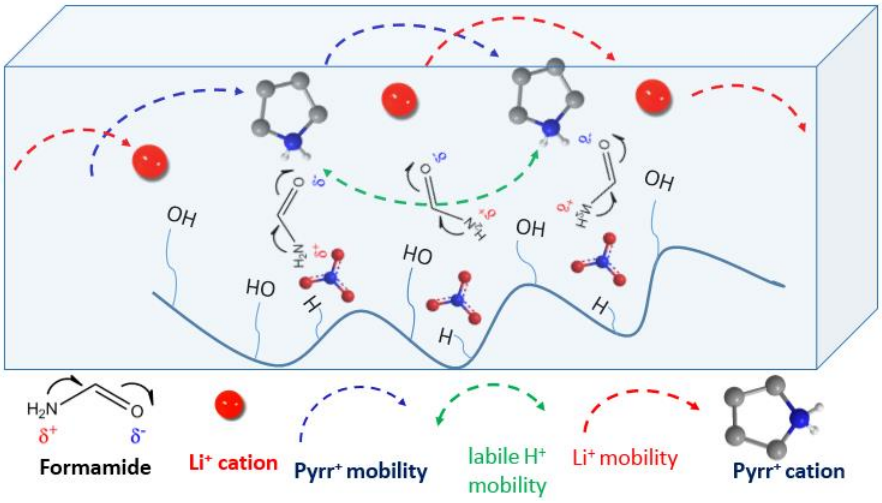

Fig.3 The illustration of ion movements in the PVA gel electrolyte

3.1.3 Lithium diffusion coefficient D_{L+} by PGSE-NMR

The gel containing both salts ($PyrrNO_3$ and $LiNO_3$) with and without FMD was analyzed by PGSE-NMR at T = 25°C. Diffusion coefficients D_{Li+} are messured and the values are almost

D_{Li+} = 7.0x10^{10}± 0.1 ms^{-1} for all samples. This indicates clearly that Li^+ ions diffused at the same level and that they were, most probably, independent to the FMD influence. We can remark also that these values are closer to D_{Li+} ions diffusion in bulk liquid [20] (D_{Li+} in LiCl ≈ 9-10 ×10^{-10} for LiCl aqueous solutions depending on the concentrations), and also higher than habitual values observed in the polymer-gel electrolyte solutions [21]. The comparison between the mobility of ions determined by the conductivity and by NMR measurements indicates that the conductive mechanism (Grotthuss) depends also on the composition of the matrix especially FMD. These high mobility values for Li^+ cannot be explained by the simple "vehicle mobility" model of ions due to the high interactions with an OH group attached to the PVA branch.

3.2 **Electrochemical Characterization of EDLC**

3.2.1 **Electrochemical impedance spectroscopy characterization**

Before the electrochemical tests, the assembled SCs were kept for several hours for a good stability. Typical the resting cell status for 3 hours is shown in Fig. 4 in which the amide systems show a quick stabilization than the bare gel based cell. This is an indication of quick cell wettability or a good interfacial stability in presence of FMD.

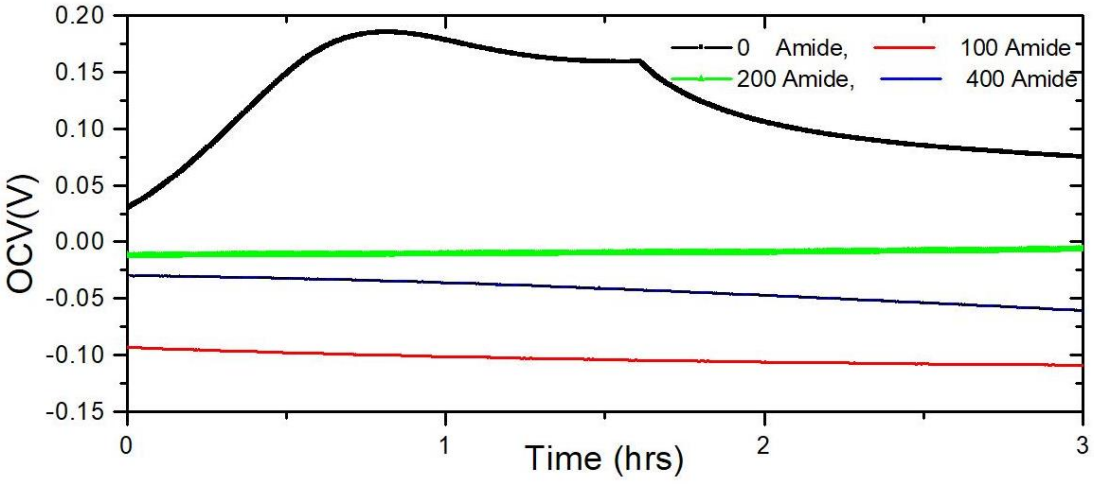

Fig. 4 The visualization of the SC's initial state of stabilizations based on amide contents in the gel

Fig.5 represents electrochemical impedance spectroscopy (EIS) results of the cells. According to the results of EIS, the cell based on the amide, 200 % (S5) has a low value of internal resistance (2.9 Ω), low polarization resistance (0.55 Ω) and low charge transfer resistance (1.5 Ω). The S4 (100 % amide) sample is similar to the S5. These results support the PVA gel, with a limit of 100-200% amide, for capacitor electrolyte applications (inset of Fig.5). Besides, the polarization resistance lowered in the case of amide electrolytes compared with the base PVA gel, is also given a positive sign to the accessibility ions at the electrodes. The solution resistances were found to be 5.0, 3.26, 3.8, 2.3, 2.8, 3.82 and 11.8 Ω for the cells S1, S2, S3, S4, S5, S6 and SA respectively

The PVA gel without ionic liquid (S1) and SA (without PVA) have more electrochemical resistive parameters, over the amide based systems. The diffusion at the electrode is better in the case of amide systems, which is confirmed by the increase of the negative coefficient of |Z| (Fig. 5b). For the S6 sample, the reverse effect is observed demonstrating the limit of the positive effect of amide adding. There was no evidence on pseudo capacitance considerations which was confirmed by the EDL type nyquist plot (charge through a phase and accumulation of charge at a phase boundary through the response of electric resistor and capacitor respectively). Specific capacitances were 24.4, 25 and 16.1 F g^{-1} for the systems S2, S4 and SA, respectively. Specifice capacitances of the cells, at 1 mHz, were deduced from the EIS and are given in Table 2. All values are given in two electrode mass basis(multiply by 4, if for the electrode specific capacitance). Charge-transfer resistances (semicircle diameter) reply the role of the PIL, FMD. The electrode and electrolyte interface is suitable for easy ionic mobilities. Furthermore, the high FMD in S6 gets more polarized than low FMD content gels.

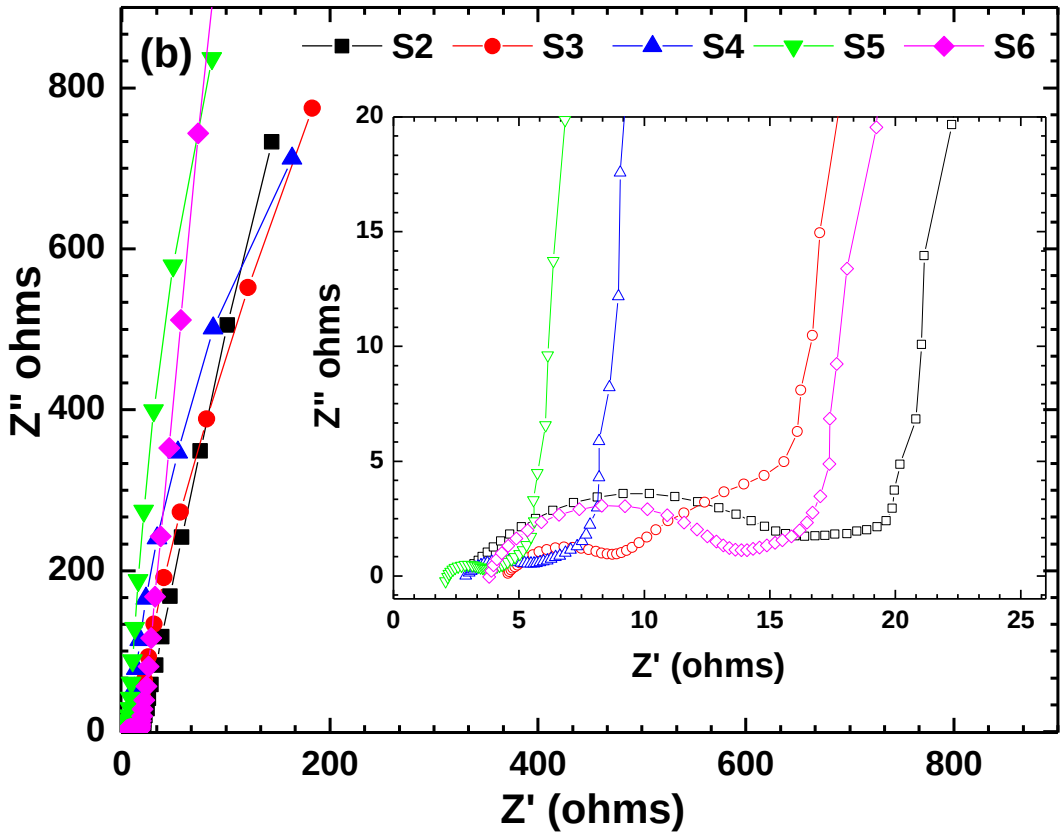

Fig. 5 Comparision of EIS spectra (Nyquist plot) of the SCs based on the GPE systems.

3.2.2 Cyclic voltammetry

The cyclic voltammetry (CV) curves of the SCs are shown in Fig. 6a and 6b at scan rates of 5 and 50 mVs^{-1} within the operational potential window of 1.5-1.75 V respectively. In the applied scan rates, there was no visible peak observed, confirms the EDL behaviors. Furthermore, good charge propagation was appeared which show good rate capability and very fast ion transportations. In addition to that, a series of current density increments were noticed by the addition of FMD, PIL over the bare GPE. It is also clearly shown that the fast ion movements were perfectly induced by the FMD. In summary, the FMD facilitates ions at higher charge applies (Fig 6b). The conductivity/internal cell resistance was reflected in the shape of the CVs in a decent order, In such cases, the low conductivity sample (SA) shows more deviation from the ideal rectangular shape than the S2 system.

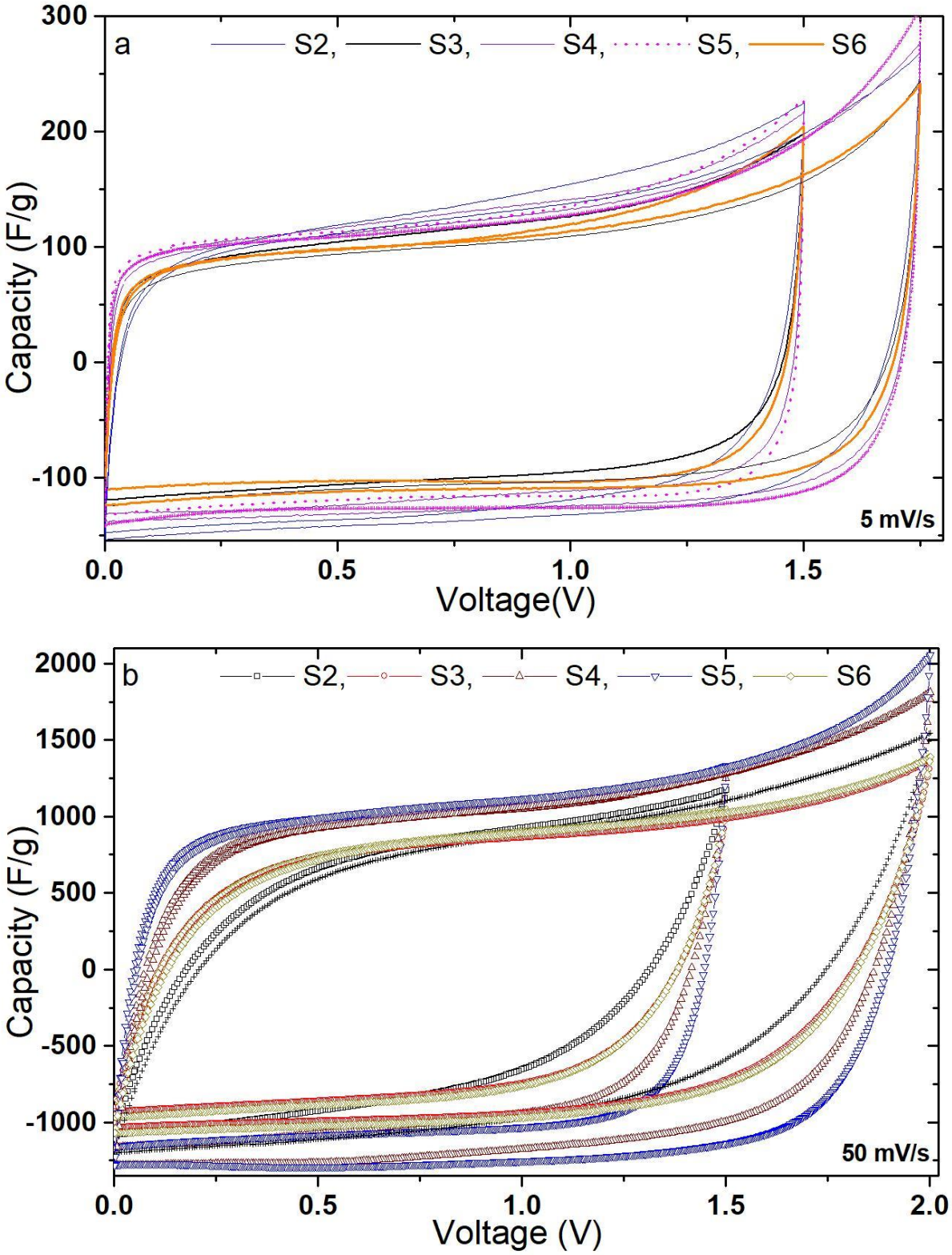

Fig. 6. CV curves of the SCs at two different scan rates; a). 5 and b). 50 mVs^{-1} in different voltage limits

The CVs exhibit EDL behavior with excellent charge propagation and the amide addition did not cause any abrupt changes to be seen in the CVs. So, the amide addition is the right choice of organic additive for the GPE. Table 2 lists some particular specific capacitance values from the CVs. The values of the SCs at 5 mVs^{-1} ranged from 25.2 to 19.2 Fg^{-1}. The amide systems were almost similar to the S2 system at low scan rate. Not much difference in the capacitance was observed between all the systems, likely the ratio of the additives to the PVA is more or less 15% only, The system SA and S6 (19.2 to 21 Fg^{-1}) present a lower capacitance value than the S2 -S5 systems (23.6 to 25.8 Fg^{-1}). The amide systems have a better capacity value and reversibility than the S2 system, especially with S5 sample containing 200 wt. % of amide. The crucial view of the amide is, there is no appreciable specific energy loss observed from low to high scan rates (25.8-23.2 Fg^{-1} from 5 to 50 mVs^{-1}) whereas the S1, S2 have merely lost a half of their capacity value. The typical range of the CVs are also useful to check the ion reversibility and ion interactions at pores of carbon in which a slow can rate involves a deep adsorption at pores, but irreversible ion kinetics that leads to its slight efficiency loss, whereas a high rate profile a deep absorption at low level pores is not influenced so leads to a small loss of capacity profile but have a good efficiency profile

Table 2. The calculated specific energy of the SCs in the GPEs from EIS and CV studies

Sample	EIS		CVs at 1.5V	
	Rs Ohm	Csp Fg^{-1}	Csp (Fg^{-1}) (5 mV/s)	Csp (Fg^{-1}) (50 mV/s)
SA	11.3	16.1	19.2	13.8
S1	5.0	23.0	24.2	13.9
S2	3.3	24.4	25.6	16.5
S3	3.8	22.8	23.6	16.6
S4	2.3	24.0	24.6	20.9
S5	2.8	25.0	25.8	23.2
S6	3.8	16.4	21.0	18.2

3.2.3 Galvanostatic Charge Discharge (CD) of the cells

For practical purposes, the SC stability and cell efficiencies during the cycling at different current densities were examined using the galvanostatic charge discharge (CD) experiments. In addition to that, cell energy and power densities were approximated by using the CD experiments. Fig. 7a represents the initial CD curves of selected SCs at a current density of 50 mAg^{-1} with a potential limit of 1.5 V. Firstly, triangular shape of CD curves is observed, which is in agreement with the capacitive behavior observed with CVs. The maximum specific discharge capacitance of the cells was obtained for S5 with 34.6 $Fg^{-1}$and a real energy density of 10.2 $WhKg^{-1}$, whereas the specific discharge capacitance and energy density of the system S2 was 20.3 Fg^{-1} and 6.36 $Whkg^{-1}$, respectively. The system SA has a low specific capacitance value (15.7 Fg^{-1}). Very similar the specific capacitance values are recorded in CV studies also (i.e., half of the cell capacity).

Furthermore, at high current densities, over all, the cell efficiencies were improved than at the low charge rates. Because of the activated carbon pore distributions, small pores could not involve the ion absorption, like high surface pores which can be seen in the low sweep rate of the CV curve at terminal voltage. Therefore, a magnified difference was noticed in the amide systems over the bare PVA system, especially considering the ohmic (IR) drop which is responsible for ionic movements. The CD curve clearly shows the perfect rectangular shape for the FMD addition. Without the FMD, CD curve deviates from the perfect curve that reply in a loss of efficiency. In order to check the possibility of the voltage window extension, SCs were carried out at 2V limit. Same results like 1.5V were observed. Especially, at the high voltage window, 2V, the amide system helps the cell to recover its efficiencies while retaining the capacitance enhancements. A typical 2 V voltage window at a charge rate of 500 mAg^{-1} is given in Fig.7b in which S5 specific capacitance was around 25 Fg^{-1} whereas, the S2 was only 18 Fg^{-1} The acquired energy density of S5 was 14.2 $Wh.kg^{-1}$with 0.43 $kW.Kg^{-1}$ power densities. Table 3 represents the performances, power and energy densities, of the cell systems at 500 $mA.g^{-1}$ with in the 2V limit. It can be observed that systems S1, S2 and SA have shown a lesser specific discharge capacitance than the amide cells. Recapabilty of charging-discharging of the cells have easily done in the case of FMD addition which supports ionic mobility in the gel surely.

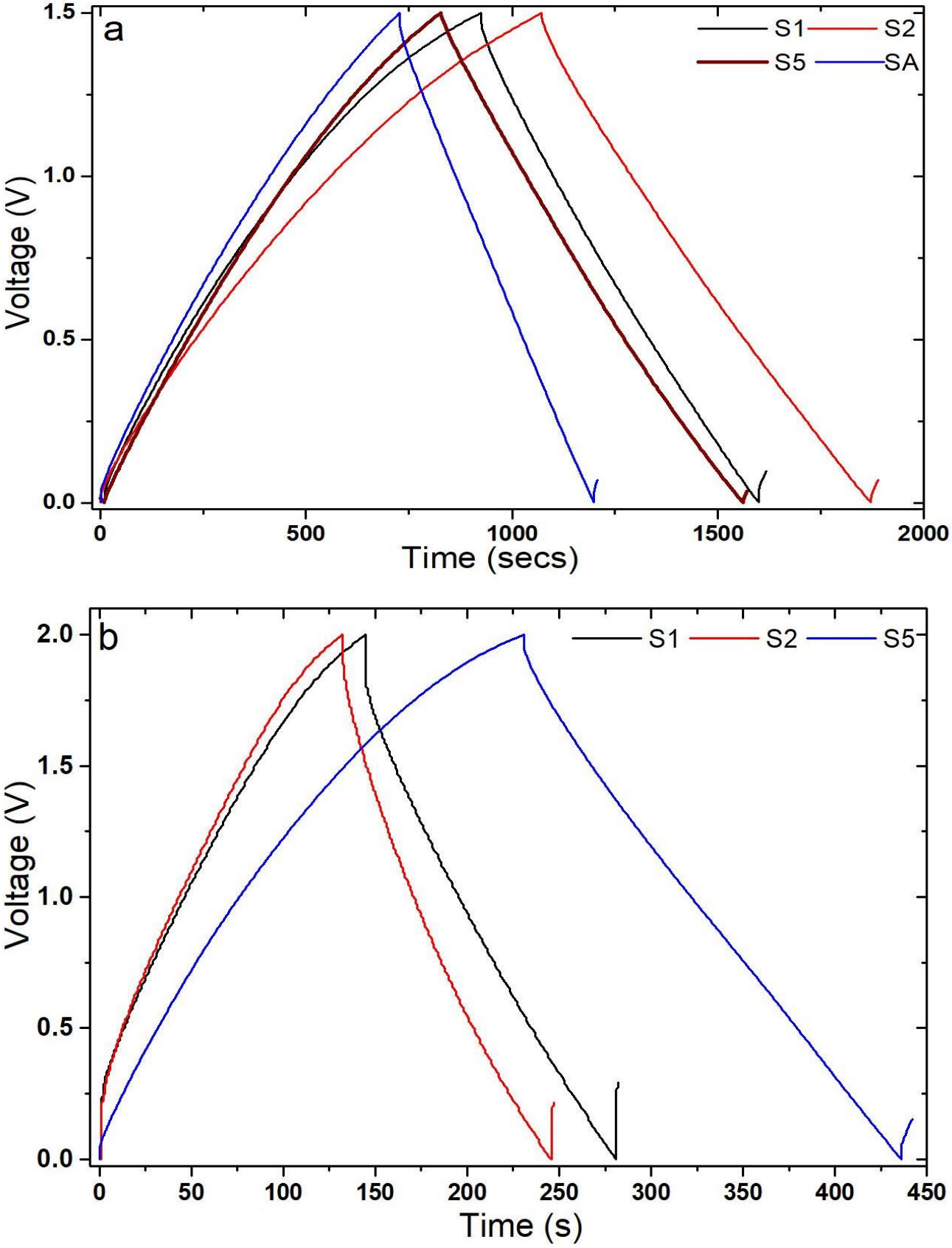

Fig. 7 The selected CD profile of the cells at current densities of 50 mAg^{-1} (Fig.7a) and 500 mAg^{-1} (Fig. 7b) at different voltge limits.

Throughout the studies, the limitation of the FMD to the gel electrolyte was clearly evidenced from the charge discharge studies with the help of the cell specific capacitance versus the content of FMD to the gel electrolyte which is shown on Fig. 8. This graph reveals that the ionic hindrance might be as a result of the strong force of the FMD on the ions as well as the presence of a more organic domain which lowers the conductivity of the medium.

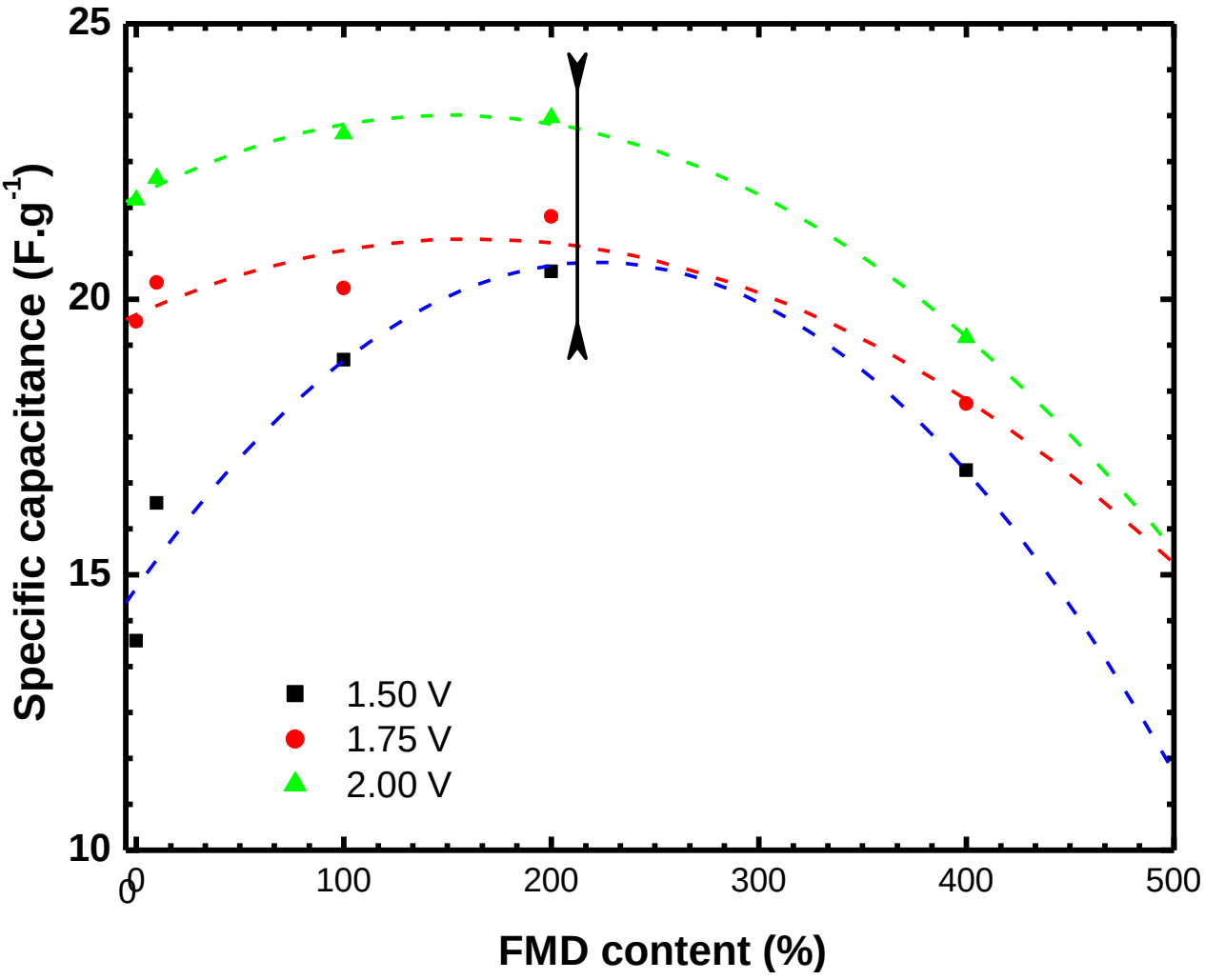

Fig. 8. The effect of amide in the gel and its limitations from the CD studies

Table 3. The calculated values of power densities and energy densities of the selected SCs systems at 500 $mA.g^{-1}$ at 2V window.

Sample	Density		5000 cycles	
	Energy Wh/kg	Power W/kg	Capacity Retention (%)	Efficiency(%)
SA	8.0	0.69	84.6	73.4/82.4
S1	8.6	0.48	69.5	70.0/78.3
S2	12.0	0.50	69.0	68.9/80.9
S3	12.3	0.51	72.5	93.5/97.8
S4	12.4	0.58	81	94.4/99.4
S5	12.8	0.56	79	92.8/98.9
S6	11.0	0.55	75.7	76.6/85.2

3.2.2 Long cycleability characterization

In order to check the capability of long cycling, the SCs were subjected to 5000 cycles at charge rate of 500 mAg^{-1}. The specific discharge capacitance versus cycle number is depicted in Fig. 9 with their corresponding efficiencies. From the results, the system S2 capacity loss is 31%, whereas, for the amide it is 21%, between the 1^{st} and the 5000^{th} cycle. This loss of capacity is appeared during the cycling is due to the saturation of the micropores with the smallest ions which is reflected in whole accessible surface area only. Beyond the 500th cycle, there is no noticeable loss was observed from 500^{th} to 5000^{th} cycles. For S1 and S2 failures, it was due to the large ohmic drops for the PVA gel systems. The cell reversibility was disturbed by the ionic motion. But, in the case of amide based gels, the amide may enhance the ion motion as observed from the conductivity and impedance studies. The curves clearly show that the bare PVA gel was not suitable for high rate cells. The system S5 and S4 exhibit the best performances and efficiency (92–94) % with capacitance of 23 Fg^{-1} for the first cycle. The corresponding calculated energy and power densities were 12.8 $Wh.kg^{-1}$ and 0.56 $kW.kg^{-1}$ respectively for S5. Additionally, for the charge rate of 250 $mA.g^{-1}$, the ohmic drops were 200, 110, 30 and 235 mV for S1, S2, S5 and SA, respectively, whereas it was 330, 190, 50, 340 mV at the charge rate of 500 $mA.g^{-1}$. Finally, the cell efficiency is a very important parameter of EDLC which was enhanced to almost 10 % from the bare PVA gel based systems by the presence of FMD

One simple way to improve the SC performance is to increase the electrolyte conductivity which was clearly confirmed by the amide inclusion in the gel. Specifically, the role of FMD fully functions in the practical SC applications.. However, it is limited one. If amide content exceeds 200 wt. % (S6), a negative effect is observed due to a strong amide interaction with the PVA gel active side

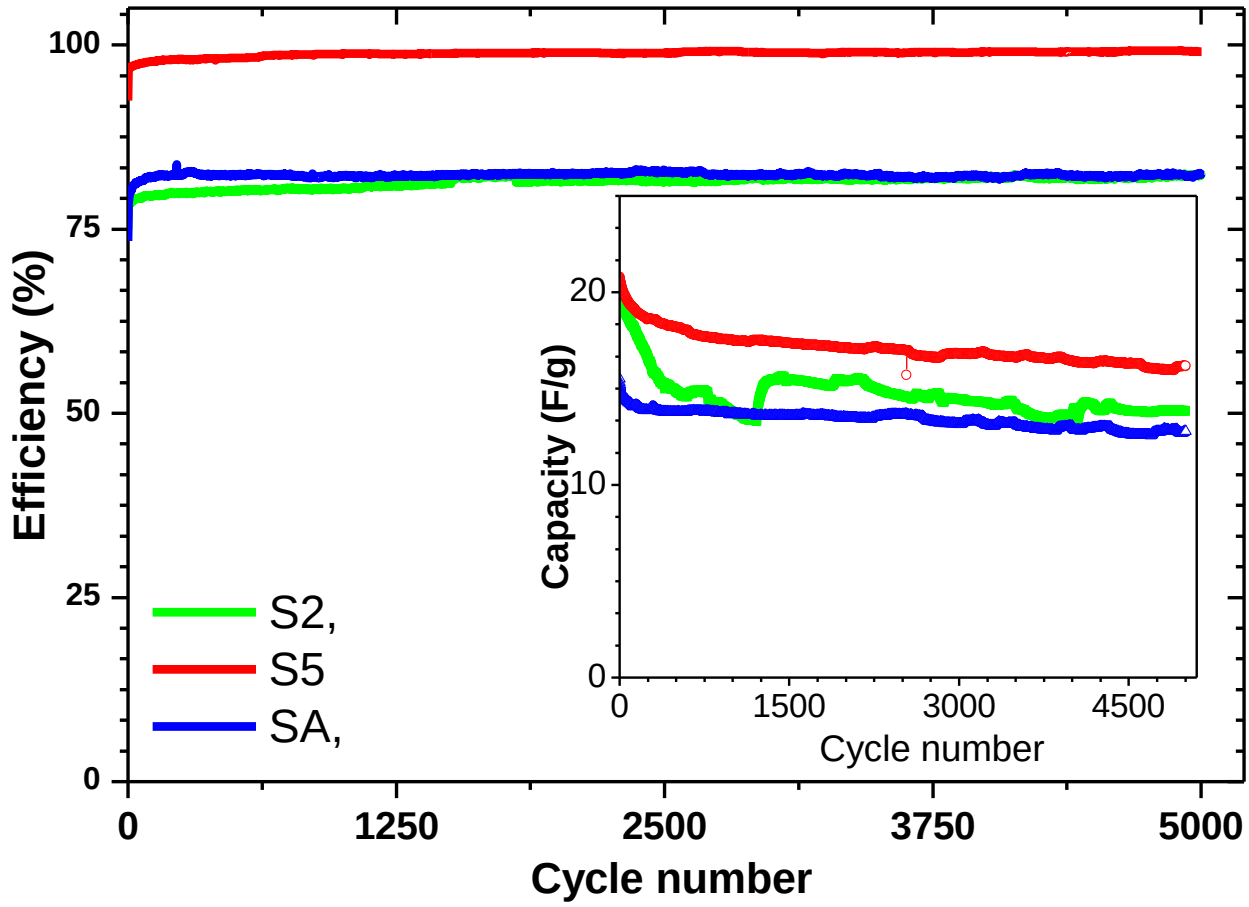

Fig. 9 Long cycling performances of the symmetric capacitors based on the gel systems SA, S2 and S5

4. Conclusions

In this work, we demonstrate that polyvinyl alcohol (PVA) in the mixture with two nitrate salts containing lithium or pyrrolidinium cation can be formulated as aqueous gel polymer electrolyte. Transport properties of these electrolytes in the presence of formamide, as an H-bond donor, demonstrates exceptional lithium mobility as well as the labile proton in the pyrrolidinium cation by Grotthuss model.This allows very large conductivities even at low temperature such as -20°C, with 11 $mScm^{-1}$ as residual conductivity. The AC-based EDLC supercapacitor supports the FMD addition for capacitor enhancements. Indeed, 200 % of amide (3 g in 30 ml water) based gel has shown a maximum ionic conductivity of 39 x 10^{-3} Scm^{-1}at 25°C. The cycle life is extended by the additive over the bare PVA gel which was evidenced by galvanostatic cycling. The specific capacitance of the cell based on the 100% of amide can be used for delivering up to 34.2 Fg^{-1} at operating voltage of 1.5 V. This quasi solid-state supercapacitor will be able to deliver an energy13-12 $Whkg^{-1}$and a maximum power of 0.56 $kWkg^{-1}$at 2.0 V. The usual capacity loss during the high C rate is minimized in the case of amide based gels which is responsible for chain flexibility during the ionic motions. So the amide based gels are much more favorable electrolyte system than that of the bare PVA gel. These promising results, stability and conductivity of the gel at -20°C permit the use of this electrolyte at low temperature also. These measurements are currently in progress in our group.

Declaration of Competing Interest

The authors declare that they have no known competing financial interests or personal relationships that could have appeared to influence the work reported in this paper.

Acknowledgments

We acknowledge the support by LE STUDIUM Loire Valley Institute for Advanced Studies, 1 rue Dupanloup 45000 Orléans – FRANCE, The author RC personally thanks to LESTUDIUM for the visiting researcher award and Universite Francois-Rabelais de Tours, Département de chimie, Parc de Grandmont 37200 Tours, France for Laboratory facilities.

References

[1] R. Chandrasekaran, J. Palma del Val, M. Anderson, An activated carbon supercapacitor analysis by using a gel electrolyte of sodium salt - polyethylene oxide in an organic mixture solvent, J. Solid State Electrochem. 18(8) (2014), 2217-2223. https://doi.org/10.1007/s10008-014-2466-3

[2] M. Zhong, M. Zhang, X. Li, Carbon nanomaterials and their composites for supercapacitors, Carbon Energy. 4(5) (2022), 950–985 https://doi.org/10.1002/cey2.219

[3] M. Maher, S. Hassan, K. Shoueir B. Yousif, M.Eldin. Abo-Elsoud, Activated carbon electrode with promising specific capacitance based on potassium bromide redox additive electrolyte for supercapacitor application, J. Mat. Res. Tech. 11(2021),1232-1244, https://doi.org/10.1016/j.jmrt.2021.01.080

[4] B. Gorska, E. Frackowiak, F. Beguin, Redox active electrolytes in carbon/carbon electrochemical capacitors, Current Opinion in Electrochem., 9(2018), 95-105 https://doi.org/10.1016/j.coelec.2018.05.006

[5] P.E. Lokhande, U. S. Chavan, A. Pandey, Materials and Fabrication Methods for Electrochemical Supercapacitors: Overview, Electrochem. Energy Rev. 3(2020), 155–186. https://doi.org/10.1007/s41918-019-00057-z

[6] W. Ye, H. Wang, J. Ning, Y. Zhong, Y.Hu, New types of hybrid electrolytes for supercapacitors, J. Energy Chem. 57 (2021), 219–232, https://doi.org/10.1016/j.jechem.2020.09.016

[7] K. S. Lee, H. T. Jeong, Development and optimization of ionic liquid based gel polymer electrolyte for all solid-state supercapacitor, J. Energy Storage, 42 (2021). 103001, https://doi.org/10.1016/j.est.2021.103001

[8] R. Chandrasekaran, J. Palma, M. Anderson, A 3-V electrochemical capacitor study based on a magnesium polymer gel electrolyte by three different carbon materials, J. Solid State Electrochem. 18(2014), 2903–2911, https://doi.org/10.1007/s10008-014-2557-1

[9] H. Dai, G. Zhang , D. Rawach, C. Fu, C.Wang, X.Liu, M. Dubois, C. Lai, S. Sun, Polymer gel electrolytes for flexible super capacitors: Recent progress, challenges, and perspectives, Energy Storage Materials, 34(2021), 320-355. https://doi.org/10.1016/j.ensm.2020.09.018

[10] S. Ujith, M. Bandarage, V.M .Sundararajan, Synthetic hydrogels: Synthesis, novel trends, and applications, J. Appl. Polym. Sci. 138(2021), 50376, https://doi.org/10.1002/app.50376.

[11] C.M. Hassan, N.A. Peppas, Structure and Applications of Poly (Vinyl Alcohol) Hydrogels Produced by Conventional Crosslinking or by Freezing/Thawing Methods, Adv.Polym. Sci. 153(2000), 37-65. http://dx.doi.org/ 10.1007/3-540-46414-X_2

[12] R. Chandrasekaran, J. Palma del Val, Marc Anderson, An electrochemical cell study on polyvinylpyrrolidine aqueous gel with glycol addition for capacitor applications, Electrochim. Acta. 135(2014), 181–186. https://doi.org/10.1016/j.electacta.2014.04.169

[13] L. Timperman, A. Vigeant, M. Anouti, Eutectic mixture of Protic Ionic Liquids as an Electrolyte for Activated Carbon-Based Supercapacitors, Electrochim. Acta, 155 (2015), 164-173, https://doi.org/10.1016/j.electacta.2014.12.130

[14] W. Zaidi, L. Timperman, M. Anouti, Deep eutectic solvent based on sodium cations as an electrolyte for supercapacitor application, RSC Adv. 4(2014), 45647–45652, https://doi.org/10.1039/C4RA08178A

[15] M. Anouti, in Electrochemistry in Ionic Liquids: Fundamentals, 1 (2015) 217-252. In: Torriero, A. (eds) Electrochemistry in Ionic Liquids. Springer, Cham. ISBN 978-3-319-13484-0 https://doi.org/10.1007/978-3-319-13485-7_7

[16] J. Pires, L. Timperman, J. Jacquemin, A. Balducci , M. Anouti, Density, conductivity, viscosity, and excess properties of (pyrrolidinium nitrate-based Protic Ionic Liquid + propylene carbonate) binary mixture, J. Chem. Thermodynamics. 59 (2013) 10–19. http://dx.doi.org/10.1016/j.jct.2012.11.020

[17] M. Anouti, M. Caillon-Caravanier, Y. Dridi, H. Galiano, D. Lemordant, Synthesis and characterization of new pyrrolidinium based protic ionic liquids. good and superionic liquids, J. Phys. Chem.B, 112 (42) (2008), 13335–13343. https://doi.org/10.1021/jp805992b

[18] X. Baokou, M. Anouti, Physical properties of a new deep eutectic solvent based on a sulfonium ionic liquid as a suitable electrolyte for electric double-layer capacitors, J. Phys. Chem. C. 119(2) (2015), 970–979. https://doi.org/10.1021/jp5110455

[19] W.S. Price, F. Hallberg, P. Stilbs, A PGSE diffusion and electrophoretic NMR study of Cs+ and Na+ dynamics in aqueous crown ether systems, Magn. Reson. Chem. 45 (2007), 152–156. https://doi.org/10.1002/mrc.1936

[20] P. Porion, A. Faugère, A. Delville, ^{1}H and ^{7}Li NMR Pulsed gradient spin echo measurements and multiscale modeling of the water and ionic mobility within aqueous dispersions of charged anisotropic nanoparticles, J. Physical Chem. C,112, 31(2008), 11893-11900. https://doi.org/10.1021/jp802928n

[21] B.E.Kidd, S.J. Forbey, F.W. Steuber, R.B.Moore, L.A. Madsenm, Multiscale lithium and counterion transport in electrospun polymer-gel electrolyte, Macromolecules 48 (2015) 4481-4490, https://doi.org/10.1021/acs.macromol.5b00573